Available online at www.HighTechJournal.org

HighTech and Innovation Journal

Vol. 1, No. 3, September, 2020

Innovative Blade Trailing Edge Flap Design Concept using Flexible Torsion Bar and Worm Drive

Kwangtae Ha [a*]

[a] *Department of Floating Offshore Wind Energy Generation Systems, University of Ulsan, Ulsan 44610, South Korea.*

Received 28 June 2020; Revised 07 August 2020; Accepted 11 August 2020; Published 01 September 2020

Abstract

In this paper, a simple but effective trailing edge flap system was proposed. This preliminary concept uses a more practical and stable actuation system, which consists of a motor-driven worm gear drive and a flexible torsion bar. The flexible torsion bar is designed to be easily twisted while keeping bending rigidity as a support, and the worm gear drive not only provides high torque to overcome aerodynamic forces on the flap area and the torsional rigidity of the support bar, but also acts as a brake to avoid instability due to the high torsional flexibility of the support bar. A preliminary level design study was performed to show the applicability of the new trailing edge flap system for wind turbine rotor blades or helicopter blades.

Keywords: Wind Turbine Rotor Blade; Helicopter Blade; Torsion Bar; Flap.

1. Introduction

Rotor blade vibrations and noise are generated during all operating conditions, primarily due to unsteady aerodynamic loads. The reduction of such vibratory loads is quite important, so much research has been performed to develop various passive and active methods and mechanisms for achieving this goal [1-3]. Also, the application of active materials for the reduction of vibration and noise in rotor blades has been the focus of numerous studies in recent years [4, 5]. From the aerodynamic point of view, the outboard region is subject to the highest values of dynamic pressure and consequently offers the greatest potential for the generation of rotor blade control air loads with minimal actuation effort (i.e., minimal deformation of the blade), as well as having the largest effect on blade loads due to large leverage. Straub et al. [6] researched trailing edge flaps with various mechanisms and actuators, and Bernhard and Chopra [7] investigated an active blade tip rotor with piezoelectric actuation using a bending-torsion actuator. However, most actuation systems use additional amplification mechanisms such as linkage systems to generate large deflections of the control surface for effective load control.

Ha and Dancila [8] proposed and analyzed a star-shaped composite cross section, which optimizes the extension-twist response. Composite star beams are an ideal solution for the frictionless tension-torsion hinge bar support of the rotor blade tip against centrifugal forces. A design level study on active wind turbine blade tips with a flexible torsion bar and piezoelectric actuation was done by Dancila et al. [9]. The high axial and bending stiffness and strength of the composite bar provide effective and frictionless support against axial (centrifugal) loads and transverse (lift and dead weight) loads, while the low torsional stiffness allows effective actuation by the coiled piezoelectric actuator. However, the suggested coiled actuator requires further research for realistic manufacturing, and current bender-type

* Corresponding author: kwangtaeha@ulsan.ac.kr

http://dx.doi.org/10.28991/HIJ-2020-01-03-01

actuators do not provide enough power to generate control surface deformation in the rotor blade and also do not provide force to constrain the support bar to avoid torsional instability. Another wind blade tip control mechanism concept was also proposed by Xie et al. [10]. It used a servo motor and a worm-gear reducer to control the folding of a wind turbine blade. Experiments with a small blade showed the advantages of reducing rotation torque and thrust through the implementation of a worm gear drive.

There were also several studies in finding what angle of attack of an equivalent rigid section will produce the same lift as a flapped section with flap deflection angle. Fehlner worked on the design of control surfaces for hydrodynamic applications and found that slope effectiveness factor was about 3.13 corresponding to 15% flap chord [11-13]. Madsen, Barlas, and Andersen developed morphing trailing edge flap system for wind turbine and demonstrated the functionality and aerodynamic performance of the flap concept. From the research, they found that 3 degree flap deflection gives the same lift change as 1 degree pitch of the whole blade system [5, 14].

In the present work, a more practical and stable actuation system, the motor-driven worm drive, is suggested to provide trailing edge flap motion and to avoid instability due to torsional flexibility of star shaped composite beam using intrinsic self-locking principle of single worm drive. A preliminary design level study was performed to show the applicability of the new trailing edge flap system for wind turbine blades.

2. Characteristic of Flexible Trailing Edge Flap System

The characteristics of the flexible torsion bar and worm gear drive, which comprise the new trailing edge flap system are briefly explained analytically.

2.1. Flexible Torsion Bar

Figure 1 shows possible redistributions of a circular cross sectional material to star configuration section and a representative flexible torsion bar with three arcs. From Equations 1 to 3, Figures 2 and 3 are obtained visually, which show that the transition improves the performance [8]. That is, it is possible to achieve a beneficial stiffness decreases in torsional stiffness and an increase in bending stiffness while keeping the axial stiffness unchanged.

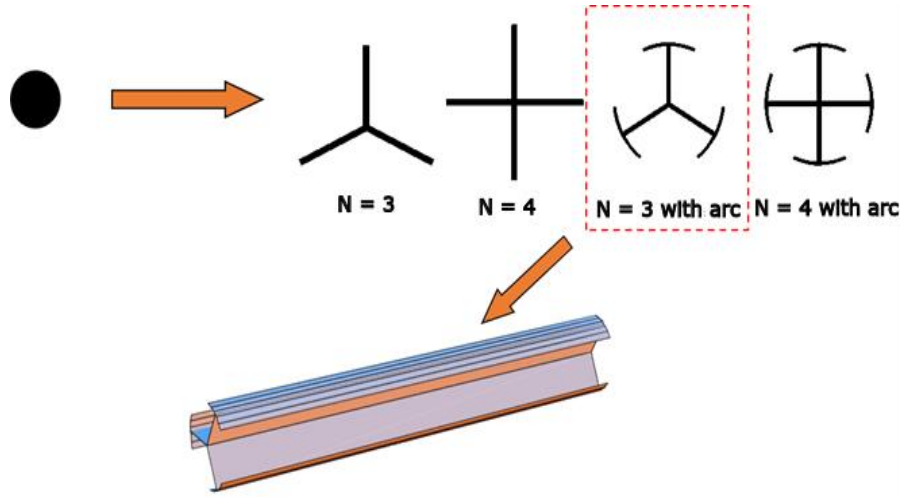

Figure 1. Redistribution of circular section to star beam and a representative flexible torsion bar

$$\frac{(EA)_S}{(EA)_{circular}} = 1 \tag{1}$$

$$\frac{(EI)_S}{(EI)_{circular}} = \frac{2\pi}{N_S\eta}\frac{\left(\frac{2\pi\phi}{N_S}+\frac{\eta^2}{12}+\frac{1}{3}\right)}{\left(1+\frac{4\pi\phi}{N_S}+\frac{4\pi^2\phi^2}{{N_S}^2}\right)} \tag{2}$$

$$\frac{(GJ)_S}{(GJ)_{circular}} = \frac{2\pi\eta}{3N_S}\frac{\left(\frac{2\pi\phi}{N_S}+1\right)}{\left(1+\frac{4\pi\phi}{N_S}+\frac{4\pi^2\phi^2}{{N_S}^2}\right)} \tag{3}$$

Where, *EA* is axial stiffness, *EI* is bending stiffness, N is the arm number of star shape, η is the ratio of wall thickness to radius of star shape cross section, $\emptyset$ is a nondimensional parameter, and *GJ* is torsional stiffness. Also, subscript s and circular represent star shaped cross section and circular solid cross section, respectively.

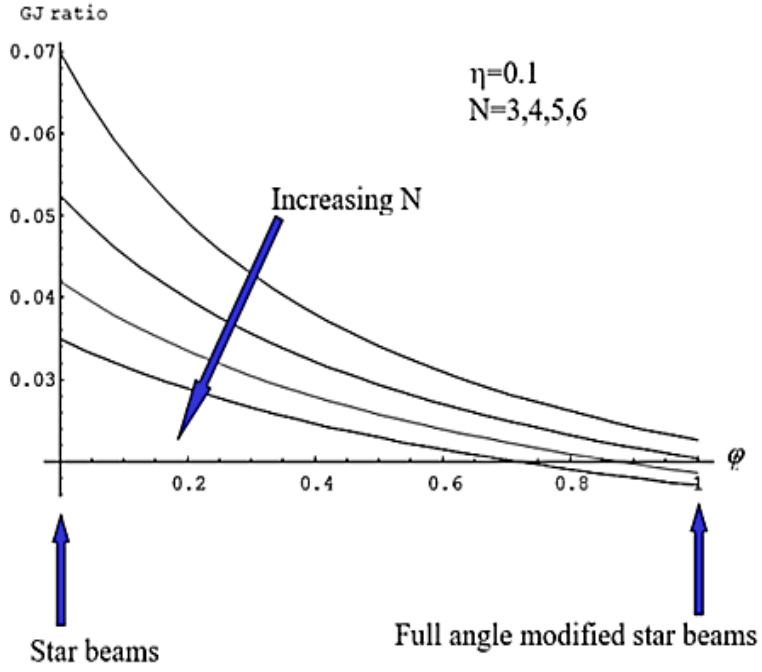

Figure 2. Variation of torsional rigidity ratio

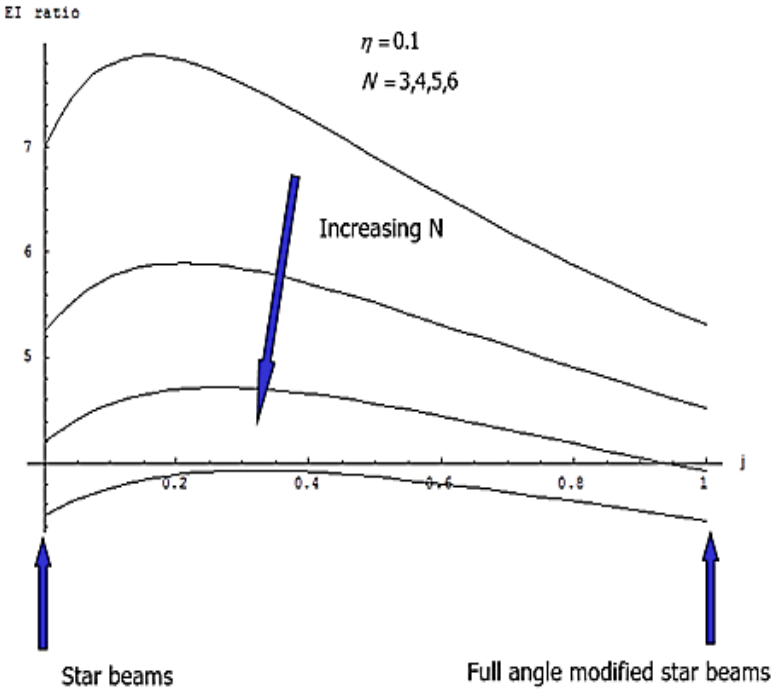

Figure 3. Variation of bending stiffness ration

Also, from Figures 2 and 3, it is shown that the torsional rigidity can be reduced to less than 7% while the bending stiffness can be increased more than seven times and the axial stiffness is preserved.

2.2. Worm Gear Drive

Figure 4 shows typical worm gears consisting of worm as the driving part and wheel gear as the driven part. It has been mainly used to applications requiring a large gear reduction, that is, a high torque with for this application, a maximum 90° motion transfer at the wheel gear end. Another interesting part is that the worm can easily turn the wheel gear, but the wheel gear cannot turn the worm reversely. This is a useful feature to the currently proposed trailing edge flap system because it keeps the flexible torsion bar from turning excessively to cause torsional instability.

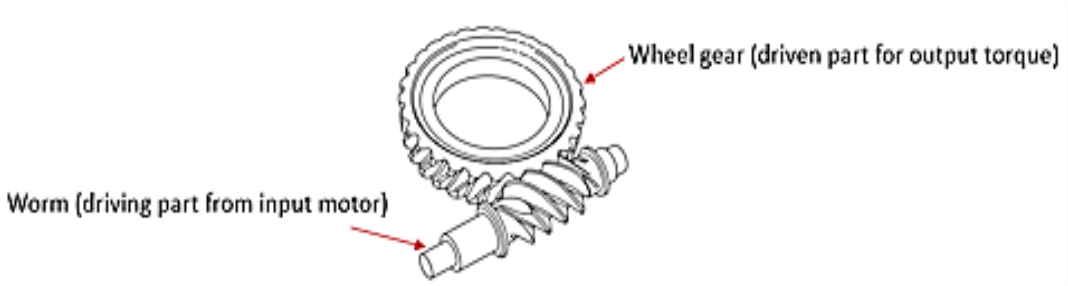

Figure 4. A schematic diagram of worm gear drive component

3. Modeling of Flexible Trailing Edge Flap System

By considering the proposed flap system subjected to combined axial loads and tip torques, the governing equations exhibiting the apparent torsional stiffening of flexible torsion bar is expressed in terms of the tip twist angle θ_s by Equation 4 [9].

$$T = \left[\frac{(GJ)_S}{L_S} + \frac{FI_S}{A_S L_S}\right]\theta_s + \frac{E_S I_{NL}}{{L_S}^3}{\theta_s}^3 = (K_{el} + K_F)\theta_s + K_{NL}{\theta_s}^3 \quad (4)$$

Where;

T : applied tip torque;

GJ : torsional stiffness;

L : longitudinal length of beam;

F : axial load;

I_{NL} : nonlinear term related to the second moment of area of the modified starbeam;

A : area of cross section;

θ : tip twist angle;

K_{el} : elastic torsional stiffness;

K_F : apparent torsional stiffness due to axial load;

K_{NL} : nonlinear term due to trapeze effect;

s : solid cross section type;

Considering the tip torque, T, at the wheel gear from worm gear drive motor, the moment equilibrium equation at the tip is given by:

$$T = T_o = \left(\frac{\omega_i}{\omega}\right)T_i = \left(\frac{\dot{\theta}_i}{\dot{\theta}}\right)T_i = [K_{el} + K_F]\theta \quad \rightarrow \quad P_i = [K_{el} + K_F]\theta\dot{\theta} \quad (5)$$

Where, P_i is a power (Watt) given from the worm gear drive motor specification, ω is a rotational speed. Therefore, the flap angle is expressed in Equation 4 with integration by parts rule in terms of input power from the worm gear drive and the torsion stiffness from the flexible torsion bar.

$$\theta = \sqrt{\frac{2P_i t}{(K_{el}+K_F)}} \quad (6)$$

Where, t is operation time by the worm gear drive motor.

4. Application to Rotor Blade

Figure 5 shows the example of a flexible trailing edge flap system application to rotor blade such as wind turbine blade or helicopter blade. For simplicity, assume that the flap hinge position is located aft to the aerodynamic center axis. In the presence of air loads, a positive nose-up rotation of the trailing edge flap device is generated by a positive aerodynamic hinge moment, which tends to amplify the flap deflection.

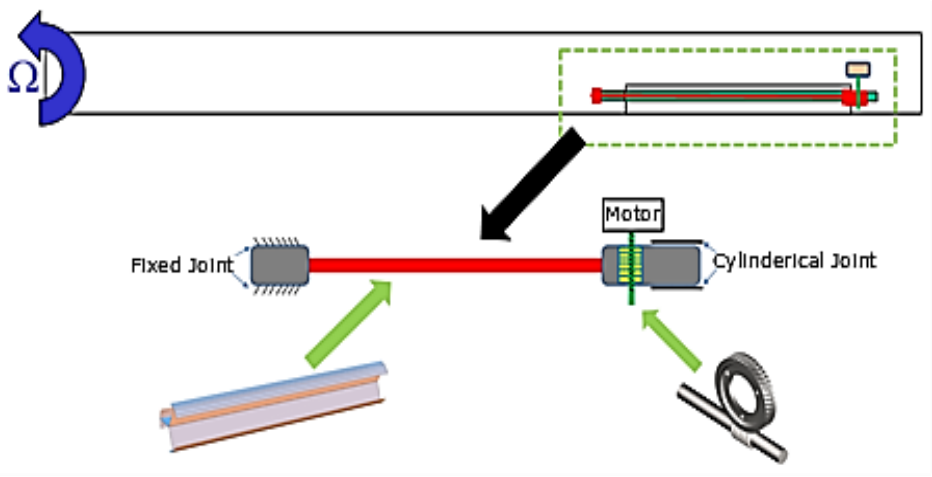

Figure 5. Schematic diagram of application to flexible trailing edge flap system on rotor blade

The equilibrium equation of the flap device at hinge location O shown in in Figure 6 becomes

$$T + M_{aero}(\alpha, \theta, \Omega) = [K_{el} + K_F]\theta \tag{7}$$

Where the aerodynamic moment is given as;

$$M_{aero}(\alpha, \theta, \Omega) = X_h L_{aero}(\alpha, \theta, \Omega) \tag{8}$$

Where;

α: Angle of attack;

Ω: Rotational speed;

L_{aero}: Aerodynamic lift force;

X_h: Distance of center of starbeam from aerodynamic center;

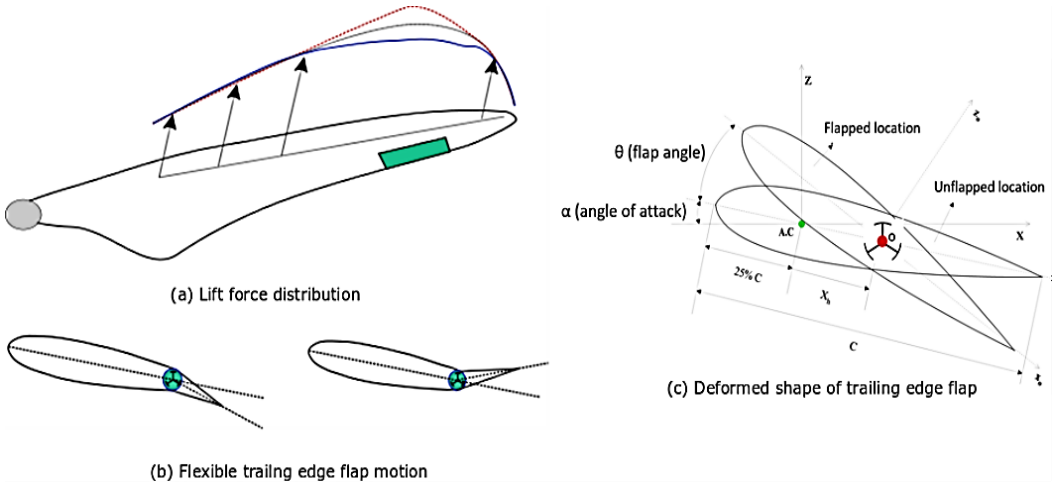

Figure 6. (a) Aerodynamic force distribution; (a) and (b) deformed cross-sectional shape of flexible trailing edge flap system

5. Conclusion

A conceptual flexible trailing edge flap system was proposed in this work. This preliminary concept uses a more practical and stable actuation system, which consists of a motor-driven worm gear drive as an input power device and a flexible torsion bar as a support bar. The flexible torsion bar showed a beneficial decrease in torsional stiffness while increasing the bending stiffness, all at the same axial stiffness as a massive bar for comparison. It was also shown that the worm gear drive not only provided high torque to overcome aerodynamic force on the flap area and the torsional rigidity of the support bar, but also acted as a brake to avoid instability due to the high torsional flexibility of the support bar. A preliminary level design study was performed to show the equilibrium condition analytically and the applicability of the new trailing edge flap system for wind turbine blades with regard to the aerodynamic force.

6. Funding and Acknowledgements

This work was supported by Brain Pool Program through the National Research Foundation of Korea (NRF) funded by the Ministry of Science and ICT (grant number: 2019H1D3A2A02102093), and this research was also supported by the Korea Institute of Energy Technology Evaluation and Planning(KETEP) grant funded by the Korea government(MOTIE) (grant number: 20184030202280).

7. Declaration of Competing Interest

The authors declare that they have no known competing financial interests or personal relationships that could have appeared to influence the work reported in this paper.

8. References

[1] Reichart, G. (1981). Helicopter Vibration Control A Survey. Vertica. 5(1), 1–20. Available online: https://dspace-erf.nlr.nl/xmlui/handle/20.500.11881/1813 (accessed on April 2020).

[2] Loewy, R. G. (1984). Helicopter Vibrations: A Technological Perspective. Journal of the American Helicopter Society, 29(4), 4–30. doi:10.4050/jahs.29.4.

[3] Barlas, T. K., & van Kuik, G. A. M. (2010). Review of state of the art in smart rotor control research for wind turbines. Progress in Aerospace Sciences, 46(1), 1–27. doi:10.1016/j.paerosci.2009.08.002.

[4] Duvernier, M., Reithler, L., Guerrero, J. Y., and Rossi, R. (2000). Active Control System for a Rotor Blade Trailing-Edge Flap, Proceedings of the SPIE Smart Structures and Materials 2000 – Smart Structures and Integrated System Conference, March doi:10.1117/12.388848.

[5] Madsen, H. A., Barlas, T., & Andersen, T. L. (2015). A morphing trailing edge flap system for wind turbine blades. In Proceedings of the 7th ECCOMAS thematic conference on smart structures and materials (SMART 2015), Azores, Portugal.

[6] Straub, F. K., Ngo, H. T., Anand, V., & Domzalski, D. B. (2001). Development of a piezoelectric actuator for trailing edge flap control of full scale rotor blades. Smart materials and structures, 10(1), 25.

[7] Bernhard, A. P. F., & Chopra, I. (2001). Analysis of a bending-torsion coupled actuator for a smart rotor with active blade tips. Smart Materials and Structures, 10(1), 35–52. doi:10.1088/0964-1726/10/1/304.

[8] Ha, K., & Dancila, D. S. (2003). Characterization of Modified Star Shape Cross-Sectional Beam Configurations with Rotorcraft Applications. 44th AIAA/ASME/ASCE/AHS/ASC Structures, Structural Dynamics, and Materials Conference. doi:10.2514/6.2003-1865.

[9] Dancila, D., Cline, J., Goss, J., Ha, K. (2010). Composite Star-Beams as Pitch Compliant Tension-Torsion Support Mechanism for Active Windmill Blade Tips, 51st AIAA/ASME/ASCE/AHS/ASC Structures, Structural Dynamics, and Materials Conference, 12-15. doi:10.2514/6.2010-2824.

[10] Xie, W., Zeng, P., & Lei, L. (2015). A novel folding blade of wind turbine rotor for effective power control. Energy Conversion and Management, 101, 52–65. doi:10.1016/j.enconman.2015.05.037.

[11] Fehlner, L. (1951). The design of control surfaces for hydrodynamic applications, Navy Department, The David W. Taylor Model Basin, Report C-358. Washington, D.C., United States. Available online: https://dome.mit.edu/bitstream/handle/1721.3/51150/DTMB_1951_C358.pdf?sequence=1&isAllowed=y (accessed on April 2020).

[12] Liu, T.-R. (2019). Quadratic feedback–based equivalent sliding mode control of wind turbine blade section based on rigid trailing-edge flap. Measurement and Control, 52(1-2), 81–90. doi:10.1177/0020294018819548.

[13] Kim, D.-H., Kwak, D.-I., & Song, Q. (2018). Demonstration of Active Vibration Control System on a Korean Utility Helicopter. International Journal of Aeronautical and Space Sciences, 20(1), 249–259. doi:10.1007/s42405-018-0106-3.

[14] Wang, F., Lu, Y., Lee, H. P., & Ma, X. (2019). Vibration and noise attenuation performance of compounded periodic struts for helicopter gearbox system. Journal of Sound and Vibration, 458, 407–425. doi:10.1016/j.jsv.2019.06.037.